Vortex formation processes from an oscillating circular cylinder at high Keulegan–Carpenter numbers

K. M. Lam,[a] J. C. Hu, and P. Liu
Department of Civil Engineering, The University of Hong Kong, Pokfulam Road, Hong Kong

(Received 15 May 2009; accepted 10 November 2009; published online 13 January 2010)

Development of vortex patterns around a circular cylinder oscillating in quiescent water is investigated using time-resolved particle image velocimetry. Experiments are performed at Keulegan–Carpenter (KC) numbers between 8 and 36 with Reynolds number kept constant at 2400. Similar to previous studies, three modes of vortex patterns are identified and denoted as modes I, II, and III. The development of vortices in each mode at successive phases of cylinder oscillation is studied in details. The classification of modes is based on the development mechanism of shear layers around the cylinder, the number of vortices shed in each half cycle, and the characteristics of the vortex street. Modes I, II, and III are characterized by one, two, and three (or more) vortices generated, respectively, in each half cycle. The appropriate vortex formation length is applied to explain the dependence of number of vortices formed in each cylinder cycle on KC. Vortex shedding in mode I occurs only on one side of the line of cylinder motion. This mode, which occurs at KC between 8 and 16, is observed to have two submodes with different orientations of the vortex street to the line of cylinder motion. Mode II occurs at KC between 16 and 24. The vortex street extends to both sides of the line of cylinder motion and lies at about 45° to it. At KC$>$24, vortices are shed behind the moving cylinder similar to the case of a towed cylinder. The limited-length vortex street in this mode III pattern lies along the line of cylinder motion. Each vortex pattern is associated with a typical secondary flow stream, which affects distinct evolution stages of vortices around the cylinder and hence the unique vortex pattern. The development of vortices is found to involve complex vortex interaction involving migration, stretching, and splitting. © *2010 American Institute of Physics*. [doi:10.1063/1.3291069]

I. INTRODUCTION

When a circular cylinder is placed in an oscillating flow, interaction occurs between the vortices shed from the cylinder and the periodic changes in flow velocities. An equivalent flow situation occurs when the cylinder undergoes an oscillatory motion in an otherwise quiescent fluid. As in studies on the starting flow past a circular cylinder, the interaction of cylinder movement with the development of shear layer in the present flow problem allows a fundamental investigation of the vortex formation process and the wake vortex patterns.[1] On the practical side, the flow is relevant to the hydrodynamic loading imposing on offshore structures, and even the design of beach processes and bed ripples.[2] The flow is governed primarily by the Keulegan–Carpenter (KC) number, $KC=2\pi A/D$, where A is the amplitude of oscillation and D is the cylinder diameter. Another parameter, namely Stokes number, is also important, $\beta=fD^2/\nu$, where f is the frequency of cylinder oscillation and ν is the kinematic viscosity of the fluid. The β parameter is actually related to the importance of the viscous effect and can also be described by the Reynolds number, $\mathrm{Re}(\equiv U_m D/\nu)$, where $U_m(=2\pi Af)$ is the maximum velocity of the cylinder movement. In fact, Re is the product of KC and β.

The flow around an oscillating cylinder is largely governed by complex vortex-structure and vortex-vortex interactions, involving the most generic phenomena of fluid dynamics, such as shear layer stability, separation, bifurcation, vortex impingement, and three-dimensional issues. Numerous investigations have been reported in the literature. One focus of investigation is the generation of fluctuating inertial, drag and lift forces on the cylinder with engineering applications to vortex-induced vibration, and loading of offshore structures (e.g., Maull and Milliner,[3] Bearman and Currie,[4] and Bearman *et al.*[5,6]). There are also investigations attempting to document the vortex patterns around an oscillating cylinder. Bearman *et al.*[5] reported some quasirepeatable vortex patterns around a cylinder placed in the oscillating flow inside a U tube. At KC$<$15, they observed a "sideway" street, which consists of successive vortices shed per half cycle and moves away from the cylinder on only one side of the line of flow oscillation. As KC$>$20 or 30, they reported a wake similar to a finite-length von-Karman street in each half oscillation cycle. Williamson[7] investigated the vortex patterns around an oscillating cylinder up to KC=60. It was suggested that the flow patterns could be grouped into four types, namely, pairing of attached vortices ($0<KC<7$), transverse street ($7<KC<15$), double pair ($15<KC<24$), and three or more pairs (KC$>$24). Similar vortex regimes were observed by Obasaju *et al.*[8] but they named the double vortex pair pattern as the diagonal regime in which a vortex pair is shed in each half cycle and is diametrically opposite

[a]Author to whom correspondence should be addressed. Fax: (852) 2559 5337. Electronic mail: kmlam@hku.hk.

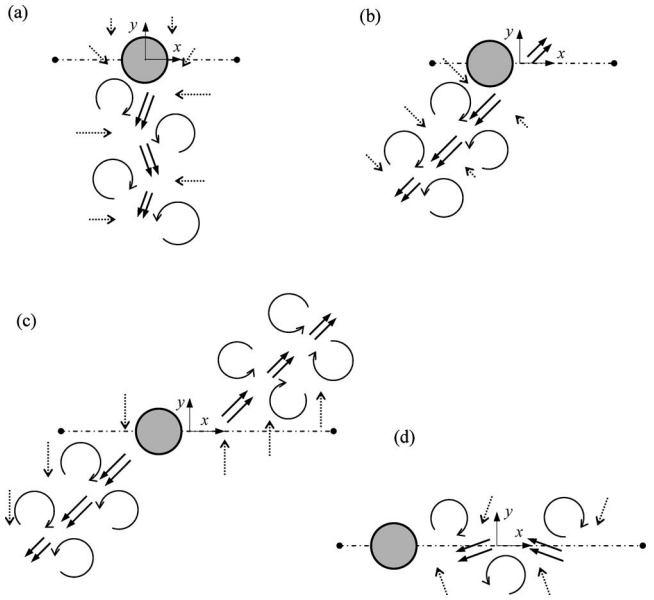

FIG. 1. Interrelation of vortex pattern with secondary flow stream. (a) Mode I, lateral vortex street; (b) mode I, inclined vortex street; (c) mode II; (d) mode III. Bold arrows: secondary flow stream; dotted arrows: ambient water flow; dot-dashed lines: typical length of cylinder stroke.

to the vortex pair in the previous half cycle. They also reported that in both the traverse and diagonal regimes, vortex pairs convect at about 45° to the line of cylinder motion.

Subsequent to Williamson[7] and Obasaju *et al.*,[8] many studies focusing on vortex patterns around the oscillating circular cylinder have been reported.[9–18] These investigations, including some detail flow mapping from particle-image velocimetry or computational fluid dynamics, have provided further evidence and information on the distinct regimes of vortex pattern at different KC ranges. Nevertheless, the exact mechanisms governing the transition of patterns remain an unresolved issue. For instance, Lam and Dai[14] studied the transition of the pattern of a vortex pair symmetric about the line of cylinder movement at small KC to the pattern of a lateral vortex street at KC=12. It is found that vortices are able to shed away from the cylinder at sufficiently high KC. Yang and Rockwell[16] found that the onset value of KC for vortex shedding is between 7 and 12.

In this paper, we apply time-resolved particle image velocimetry (PIV) to explore the vortex dynamics in details at $8<\mathrm{KC}<36$. By using the same experimental setup for the wide range of KC and the flow mapping capacity of time-resolved PIV, we aim to investigate and resolve the exact role of KC increase in determining the vortex patterns. This is the main objective and the value of this paper.

At $\mathrm{KC}>8$, vortices are shed and convected away from the oscillating cylinder.[7,8] The vortex regimes at the "high" KC numbers in this study, $8<\mathrm{KC}<36$, consist of different distinct patterns of vortex pairs shed from the oscillating cylinder. The high KC flow also has more engineering importance because the flow is drag dominated whereas it is inertia dictated at a small KC.[19] We observed the same vortex regimes as previous observations and in this paper, the vortex patterns are named modes I, II, and III for easy reference. The modes are based mainly on the number of vortex pairs shed from the cylinder in one oscillation cycle and the vortex patterns typical of each mode are sketched in Fig. 1. Mode I occurs at KC between 8 and 16. One vortex is shed from the cylinder every half cycle or every cylinder stroke. The contrarotating vortices from two successive strokes form a vortex street on one side of the line of cylinder motion only. The street is aligned approximately lateral to the line of cylinder motion at most of the time at $\mathrm{KC}\leq 12$. This is the regime of traverse vortex street reported by Williamson.[7] At higher KC, the street is sometimes aligned at roughly 45° to the line of cylinder motion, as has been observed by Obasaju *et al.*[8] At KC between $16\leq\mathrm{KC}\leq$ and 24, we observed the mode II pattern which is the double pair pattern[7] or the diagonal regime[8] reported in previous studies. Mode III occurs at $\mathrm{KC}>24$. Three or more vortices are formed every half cycle and the vortices lie mainly on the line of cylinder motion. As in published studies,[5,6] the number of vortices formed in each half cycle equals the lower bound of KC in each mode divided by 8. The PIV velocity data presented in this paper for modes II and III have not been reported in the literature.

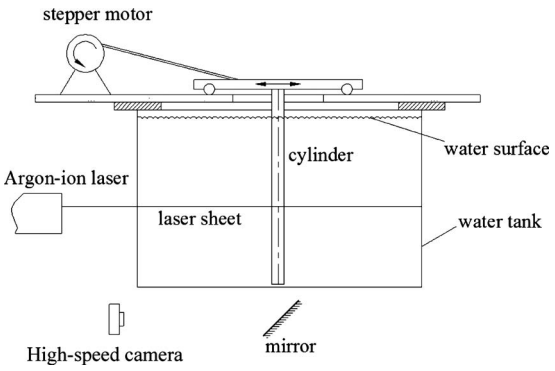

FIG. 2. Experimental arrangement.

Also included in the sketches of Fig. 1 is the flow of fluid associated with the vortex patterns in each mode. These secondary flow streams have been noted by Williamson[7] and Tatsuno and Bearman,[9] but their formation and relationship to the vortex pattern have not been examined in details. At KC=12, Lam and Dai[14] discussed that the sustainability of the lateral vortex street depends on the secondary flow stream which exists on only one side of the line of cylinder movement. There are evidences that the secondary flow stream affects the formation location of a vortex on the cylinder surface and helps to move the vortex around the cylinder surface leading to the asymmetric pattern of the lateral vortex street. In this study, we also aim to study the characteristics of secondary flow stream associated with the different vortex patterns.

II. EXPERIMENTAL DETAILS

The experiment was conducted in a water tank measuring 120×180 cm^2, with water depth filled to 50 cm. Figure 2 shows a sketch of the setup arrangement which was similar to that described in Lam and Dai.[14] A sliding table, resting on two tracks through linear bearings, was horizontally placed

above the tank. A stepper motor along with a crank yoke was employed to generate a sinusoidal motion of the sliding table as well as a rigid cylinder, which was vertically cantilever mounted on the table. To minimize three-dimensional and end effects, the gap between the cylinder end and the tank bottom was held at only about 1 mm. The amplitude of cylinder oscillation was set by the length of crank yoke while the oscillation period was controlled precisely by the speed of the motor. The motion of the cylinder was checked to follow nicely the equation $x(t)=A\sin(2\pi t/T)$, where t is time and $T(=1/f)$ is the period of one oscillation cycle. The largest deviations of the cylinder positions found from the PIV images from the ideal positions in the sinusoidal motion occurred when the cylinder was near its neutral position but the deviations at most KC numbers were within $\pm 0.1D$. The coordinate system (x,y) is defined with the origin set at the center of the cylinder in its neutral position. Coordinates x and y are along and lateral to the line of cylinder oscillation motion, respectively, whereas coordinate z is along the spanwise direction of the cylinder.

In most previous experimental studies, flow patterns at different KC numbers have been obtained in experiments at different Re.[14] To avoid the effect of viscous actions on the flow pattern, it was decided in this study to carry out all experiments at a constant Re=2400. It has been suggested that Re=2400 is sufficiently high for viscous effect to be negligible and the vortex pattern is independent on β.[14] Experiments were made with a circular cylinder of $D=20$ mm at ten values of KC between 8 and 36. To maintain a constant Re, the β parameter (or equivalently, the frequency of cylinder oscillation, f) needed to be adjusted in an inverse manner with the change in KC (or equivalently, the amplitude of oscillation, A). Thus, when KC was varied from 8 to 36, β changed from 200 to 67, respectively. The ranges of cylinder amplitude and oscillation period were, respectively, from 19.1 to 86.0 mm, and from 0.75 to 3.38 s. The maximum cylinder velocity was constant at $U_m=0.16$ m/s.

In order to quantitatively study the different vortex patterns, time-resolved PIV measurements were made. A thin laser sheet was generated by an argon-ion laser with power at about 3 W and was directed by a set of mirrors to illuminate the horizontal plane passing through the midspan of the vertical cylinder. The flow was seeded by neutrally buoyant synthetic polycrystalline particles of about 30 μm in diameter. With the continuous wave laser and the slow flow velocities, we could manually observe the movements of seeding particles and visualize the existence of a particular vortex pattern. After a test run, the cylinder oscillation was stopped and the next test run was started only after we had confirmed visually that there was no residual motion of water in the tank from the previous test. With originally quiescent water in the tank, the cylinder was given the prescribed oscillatory motion. After some cycles, usually less than 10, when we could visually observe that a periodic vortex pattern was sustained, image recording was started. A time sequence of PIV images on the (x,y) plane was captured by a high-speed camera (PCO 1200 hs) at a rate of 100 image/s. The exposure time of each image was set at 8 ms. An optical filter was used to allow only the green laser light scattered by the seeding particles to pass. Around 5000 PIV images were acquired for each KC number. This lasted for many cylinder oscillation cycles and at some KC, the flow might switch between two or more different vortex patterns during the recording period. The distinction of vortex patterns in each cylinder oscillation cycle was made from the PIV results in the postprocessing. There was time stamping on each image so that it is possible to correlate the vortex pattern with the cylinder position. We focus on the flow structures in the (x,y) plane, although three dimensionality has been noted at the present Reynolds number.[12]

Particle images recorded on two consecutive images were analyzed by a PIV analysis software (DANTEC DYNAMICSTUDIO V2.10). The analysis was based on the spatial cross-correlation algorithm of Willert and Gharib[20] but with adaptive and multipass interrogation windows. All velocity vectors were validated with a threshold of signal-to-noise ratio at about 1.2 for the correlation peaks. Rejected vectors were replaced by vectors estimated from the surrounding values. In the final iteration, PIV vectors are obtained on interrogation areas of size 32 pixels $\times$ 32 pixels and with 50% overlap. With the camera resolution at 1280 pixels $\times$ 1024 pixels, the two-dimensional velocity field at each time instant consisted of 79×63 vectors of U and V (4977 vectors in total). In most test runs, this spatial resolution of 16 pixels corresponded to roughly 2 mm or $0.1D$. For the temporal resolution, the time interval between consecutive PIV snapshots was 10 ms. From the values of T at different KC, this means that there were 75–338 snapshots in one cylinder oscillation cycle. The PIV system thus provided sufficiently fine temporal and spatial resolution for the investigation of vortex formation from the cylinder. From the velocity vectors, spanwise vorticity component ω_z was computed.[21] Experimental uncertainties in determining the velocities and spanwise vorticity were estimated to be 5% and 7%, respectively.

III. RESULTS AND DISCUSSION

Experiments have been made at ten values of KC at KC=$\{8,10,12,14,16,20,24,28,32,36\}$, but we shall discuss the results at some selected values of KC. We shall show later that it is advantageous to discuss the flow interaction at various cylinder positions using the cylinder stroke. One cylinder stroke is the traverse (rightward or leftward) of cylinder movement. A stroke length is $2A$ or $1/\pi$ (KC) D and it lasts for one half cycle. During one cylinder stroke, one, two, and three (or more) vortices are generated for modes I, II, and III, respectively.

A. Mode I pattern

Mode I occurs at KC between 8 and 16. It has been reported in the literature as the transverse vortex street or single vortex pair.[7–9] A vortex street is present on only one side of the line of cylinder motion (Fig. 1). It is noteworthy that either side is equally possible because the vortex street intermittently swaps from one side to the other. It has been found that below a critical KC number at KC$\approx$8, no large-scale vortices can be completely shed from the cylinder.[16]

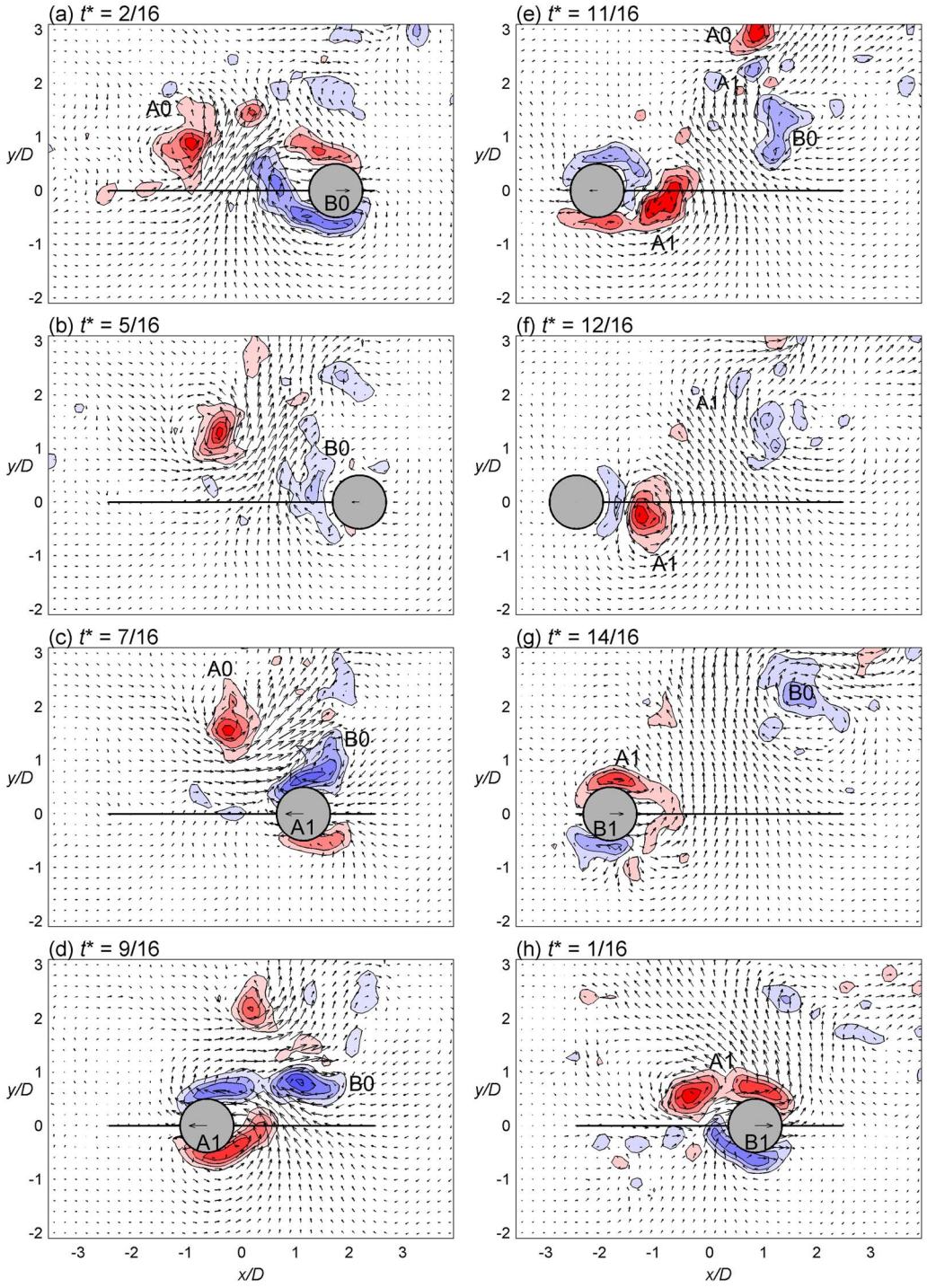

FIG. 3. (Color online) Instantaneous PIV velocity vectors and vorticity contours at successive phases of cylinder movement of mode I at KC=16. Vectors are shown on coarser grid for clarity. Instantaneous cylinder velocity is shown on cylinder in each plot. Cylinder speed at $t^*=7/16$ is $0.924U_m$. Vorticity contours in $\omega_z^*=\pm1,\pm2,\pm3,\ldots$.

Only small vortices are found to remain attached to, or detached for a short distance from, the cylinder surface.[7–9,14] Mode I is observed when KC number is sufficiently large (KC>8) to allow shedding of large-scale vortices from the cylinder.

In the present study, we observed that the vortex street is not necessarily always perpendicular to the line of cylinder motion. Sometimes, the vortex street is aligned at about 45° to the line of cylinder motion [Fig. 1(b)]. In the present study, this submode is observed to occur more often at KC>12. The same submode was reported in Williamson[7] as the single (vortex) pair. We shall first present PIV results at KC=16 at which occurrence of the two submodes of mode I, and even mode II, is observed to be possible.

The development and shedding sequence of vortices from the cylinder to form an inclined vortex street in mode I is explained with the help of Fig. 3. The figure shows the instantaneous PIV snapshots at some selected phases over

two consecutive cylinder oscillation cycles. The velocity vectors and vorticity contours are shown in each PIV snapshot. For clarity, the original set of PIV vectors on a fine grid of $0.1D$ resolution is not shown and interpolated vectors on a coarser grid at $0.2D$ resolution are shown instead. Throughout this paper, we use the asterisk to denote nondimensional quantities which have been normalized using characteristic scales such as T, U_m, and D. Therefore, the phase of cylinder movement is represented by $t^*=t/T$. The phases in Fig. 3 and subsequent similar figures are denoted as 1/16 fractions of one cycle but the phase resolution in our time-resolved PIV measurements is much finer in the order of hundreds of phases per cycle. The vortex contours are those of the nondimensional spanwise vorticity, $\omega_z^*=\omega_z D/U_m$. For clarity, contours of vorticity levels close to zero are not shown.

We first look at the PIV snapshot in Fig. 3(c) at phase $t^*=7/16$ in the first cycle. The cylinder is in the first half of its leftward stroke. On its upper surface, a clockwise rotating vortex B0 remains attached to the cylinder. This vortex is formed from the previous rightward stroke and is about to be shed from the cylinder. On the lower side of the cylinder, there is a counterclockwise vortex A1. This new vortex is rolled up when the cylinder starts the present leftward stroke. During the stroke, it grows with vorticity fed from the lower shear layer of the cylinder. When the cylinder moves past its neutral position, the mature vortex B0 on the upper side of the cylinder is shed behind the moving cylinder near $t^*=9/16$ [Fig. 3(d)]. Associated with the shedding of B0, vortex A1 is observed to move upward toward the line of cylinder motion [Figs. 3(d)–3(f)]. A detailed discussion of this migration of A1 will be given later in this section. At the end of the leftward stroke, vortex A1 has been migrated almost above the line of cylinder motion [Fig. 3(f)].

When the cylinder reverses its moving direction and travels rightward in the next stroke, vortex A1 is brought to the cylinder upper surface [Fig. 3(g)]. During the first half of this rightward stroke, vortex A1 continues to be fed vorticity of the positive sign but now from the upper shear layer instead of the lower shear layer. The vortex thus grows into a mature stage of strong circulation. It is shed behind the fast moving cylinder where the cylinder has passed its neutral position in Fig. 3(h) at $t^*=1/16$ of the second cycle. Its location upon shedding is near $(x,y)=(0,0.5D)$.

At the same time, when the cylinder starts this rightward stroke, a new clockwise rotating vortex B1 is formed from the rollup of the shear layer at the lower side of the rightward-moving cylinder. We can observe the development of this vortex subsequent to Figs. 3(g) and 3(h) from the clockwise vortex B0 formed in the previous cylinder cycle in Fig. 3(a). The evolution stages of this vortex are similar to those of vortex A1 in the previous stroke except for the difference sense of vortex rotation and direction of cylinder movement.

At the end of the rightward stroke, we can observe that the clockwise vortex B0 in Fig. 3(b) has moved above the y-axis. The vortex is subsequently shed behind the leftward-moving cylinder on passing its neutral position [Figs. 3(c) and 3(d)]. The vortex center upon shedding is located near $(x,y)=(1.5D,0.6D)$ and the shed vortex B0 forms a vortex pair with vortex A0, which developed one stroke earlier. The vortex pair is located offset to the right side of the cylinder neutral position and between them is a strong secondary flow stream, which is flowing upward at about 45° to the $+y$-axis. In the subsequent phases in Fig. 3, we can observe the convection of this vortex pair away from the line of cylinder movement along the same inclined path. The next vortex pair of vortices will be formed from A1 and B1 in Fig. 3(h) after B1 is later shed from the cylinder in the following leftward stroke. This leads to the formation of an inclined vortex street, as shown in Fig. 1(b).

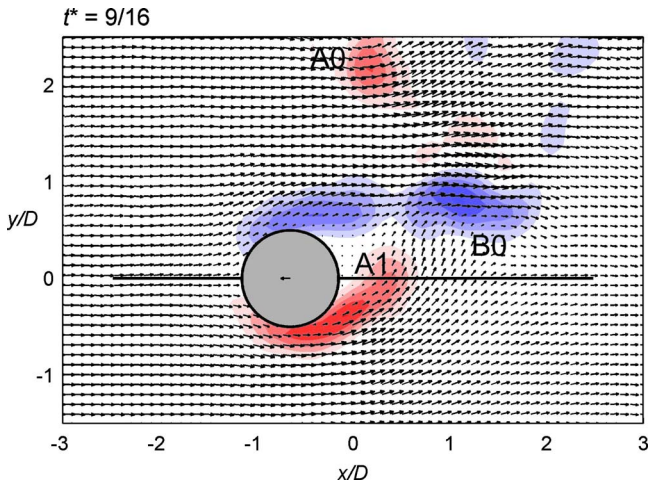

FIG. 4. (Color online) PIV velocity vectors relative to moving cylinder at $t^*=9/16$. Mode I at KC=16. Instantaneous cylinder speed at $0.924U_m$ is shown on cylinder. See Fig. 3(d) for vorticity levels.

The velocity vectors shown in Fig. 3 are relative to the otherwise stagnant water in which the cylinder undergoes the oscillation motion. We can obtain a clearer picture of the flow around the moving cylinder, especially during the shedding of a vortex, by plotting the velocity vectors relative to the instantaneous cylinder velocity. Figure 4 shows these relative vectors near the instant of shedding of vortex B0. They correspond to the absolute velocity vector maps in Fig. 3(d) but PIV vectors on the original grid resolution are shown. The inclusion of the cylinder velocity does not affect the vorticity field. It is observed in Fig. 4 that the relative velocity vectors extending from the lower side of the cylinder are almost parallel to the orientation of the positive vorticity region of vortex A1. We can now observe how the induced upward flow manifested in Fig. 3(d) brings vortex A1 to intrude into the region of opposite vorticity on the upper shear layer of the cylinder and break off vortex B0 from the shear layer. This observation agrees with the findings of Cantwell and Coles[22] that the shedding of a vortex is aided by the intrusion of the opposite-signed vortex from the other side of the body from behind which cuts off the vorticity supply to the shedding vortex from its shear layer.

In the vector maps of absolute velocities in Fig. 3, a strong upward-flowing secondary flow stream is observed between vortices A0 and B0 for the latter part of the leftward stroke. Lam and Dai[14] suggested that this flow stream has the effect of migrating vortex A1 upward around the trailing surface of the cylinder. However, the present findings of Fig. 4

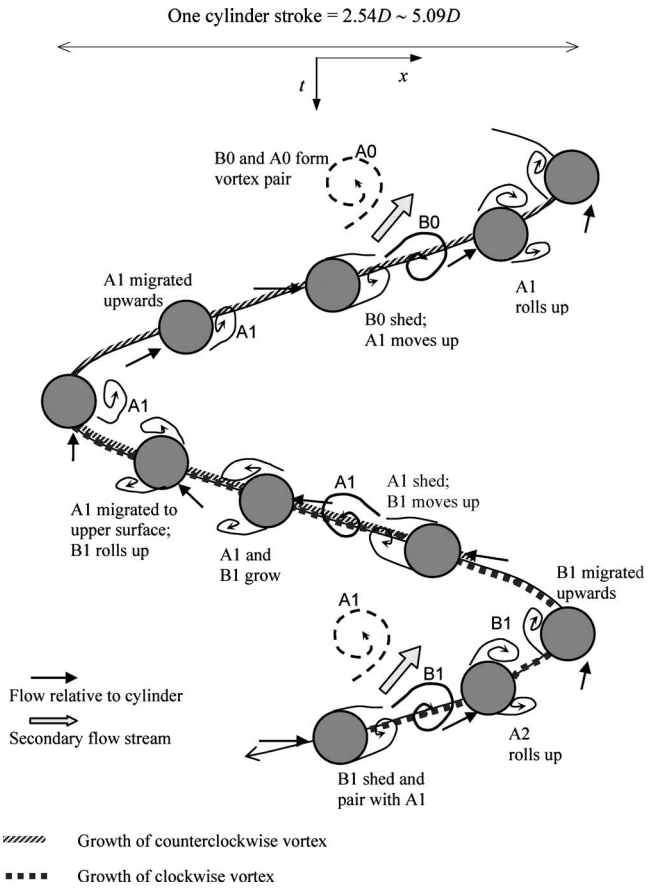

FIG. 5. Development stages of vortices in mode I.

suggest that the upward migration of vortices from the lower side of the cylinder may be triggered in the first place by the natural shedding mechanism of vortices from the upper shear layer.

The development stages of the vortices in mode I are sketched in Fig. 5. This is for the submode of a vortex street existing above the line of cylinder motion and inclined at about 45° to the $+y$-axis, as revealed in Fig. 3. All vortices of the street originate from the rollup of the shear layer at the lower side of the cylinder at the start of every stroke. During the stroke, the vortex grows with the feed of vorticity from the shear layer. Near the middle of the stroke, a vortex of the opposite sense of rotation is shed from the upper side of the cylinder. Connected with this shedding, the vortex on the lower shear layer moves upward around the leeward side of the cylinder surface. When the cylinder traverses its next stroke, the vortex is eventually brought to the upper cylinder surface and vorticity is fed to it from the upper shear layer instead. The vortex grows to maturity and is subsequently shed into the wake above the cylinder near the middle of the stroke.

The growth time or distance of each of the two vortices in a vortex pair is sketched in Fig. 5. The growth of vortex A1 from rollup to shedding covers the leftward stroke and more than half of the following rightward stroke. The growth of vortex B1 covers a short distance including the rightward stroke and approximately the first quarter of the next leftward stroke. Jeon and Gharib[1] discussed the formation time of a vortex for shedding from a circular cylinder and used the equivalent traveling distance to denote the vortex formation time. It was suggested that around a time of $4.8D$, a vortex grows to reach a critical circulation and shedding occurs. At the present case of KC=16, the distance of $4.8D$ is equal to 0.94 stroke length. This means that a vortex can grow to maturity within one cylinder stroke. On examining Fig. 3 carefully, we can observe that at the end of the leftward stroke in Fig. 3(f), vortex A1 has grown to a mature vortex and seems to be detached from the cylinder already. However, the cylinder reverses its moving direction shortly and vortex A1 is brought to the cylinder surface again. The vorticity contours suggest that it is connected to the upper shear layer of the cylinder in its rightward stroke. This may lead to feeding of more vorticity into the vortex. The overgrown vortex is eventually shed from the cylinder shortly after the cylinder passes its neutral position with the maximum speed.

The clockwise rotating vortex B0 follows similar development stages as vortex A1 but with a shorter growth time. The velocity vectors in Fig. 3(c) suggest that the earlier shedding of B0 seems to be triggered by the interaction with vortex A1 which is located at $x \approx 0$. As will be shown later for mode II, the vortices on the obtuse angle side of the inclined vortex street, that is, A0 and A1, possess higher levels of peak vorticity as those on the acute angle side, such as vortices B0 and B1.

Mode I has another submode in which the vortex street lies almost lateral to the line of cylinder motion. At KC=16, this submode is less frequent than the other submode of an inclined vortex street. Our PIV results capture this submode at KC=16 over a few cycles (snapshots not shown for brevity). It is observed that the clockwise and counterclockwise vortices follow the same stages and time spans of vortex dynamics and development. Shedding of a vortex is observed to occur near the instant when the cylinder passes its neutral position with the maximum speed. Each vortex, clockwise or counterclockwise rotating, alike, has undergone a vortex formation time of 1.5 stroke lengths before shedding. The development stages are similar to the steps sketched in Fig. 5 but the symmetric situation leads to a pair of vortices of equal strength, which are subsequently convected away from the line of cylinder motion as a vortex street lying lateral to the line.

At a lower KC, say, KC=12, the submode of a lateral vortex street occurs for almost all cylinder cycles. The vortex patterns and dynamics have been studied in details previously,[14,23] where it was found that the lateral vortex street at KC around 12 is highly periodic and regular. Here, we use the vortex formation time of Jeon and Gharib[1] to provide an explanation for this observation. The stroke length at KC=12 is only $3.8D$, thus at the end of a stroke, a vortex has not grown to maturity. As an example, Fig. 6(a) shows the PIV snapshot at the end of a rightward stroke of the cylinder at KC=12, where a lateral vortex street is located at $y<0$. The clockwise vortex formed during this stroke is now migrated from the upper side of the cylinder to the left end of the cylinder. When compared with similar snapshots in Fig. 3 for KC=16, the vortex is clearly observed to remain attached to the cylinder. The growth of the vortex

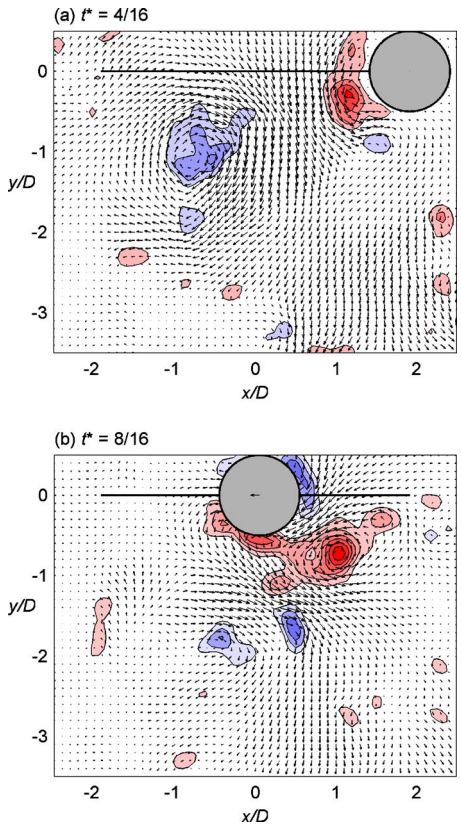

FIG. 6. (Color online) Formation of lateral vortex street at KC=12. Maximum cylinder speed U_m is shown on cylinder in (b). Vorticity contours in $\omega_z^*=\pm 1.5, \pm 3.0, \pm 4.5, \ldots$.

continues after migration to the lower surface of the cylinder when the cylinder changes its moving direction. The vortex is eventually shed shortly before the cylinder moves to its neutral position in Fig. 6(b). At this KC=12, the normal vortex formation length[1] at $4.8D$ corresponds to 1.26 stroke lengths. This means that the vortex in Fig. 6 undergoes a normal growth time and is shed naturally. The counterclockwise vortex, which is formed in the leftward stroke, also undergoes a normal growth and shedding. The appropriate value of cylinder stroke length at KC=12 enables natural growth of the vortex formed in every stroke. Each vortex grows to the same normal strength and is shed shortly before the cylinder passes its natural position in the following stroke. This results in a highly ordered and symmetric vortex street lying lateral to the line of cylinder motion.

B. Mode II pattern

Mode II occurs at a higher KC number, as compared with that of mode I. As a consequence of a larger cylinder amplitude, one more vortex is generated during each half cycle and the vortex street is present on both sides of the line of cylinder oscillation. Successive vortex pairs move away from the line of cylinder motion and two vortex streets are found in two opposite quadrants of the flow region [Fig. 1(c)]. Similar to previous studies[7,8] which denoted the vortex pattern as the double pair or the diagonal regime, we observe this mode of vortex pattern at KC between 16 and 24.

At KC=16, mode II is observed only for a small portion of the time and the oblique vortex street submode of mode I is the dominant mode. Figure 7 shows the PIV snapshots at some selected phases of a typical cylinder oscillation cycle at KC=16, where the mode II vortex pattern occurs. In Fig. 7(a), when the cylinder is near the middle of a rightward stroke, a clockwise vortex A1 is observed on the lower surface of the rightward-moving cylinder. As will be described later, this vortex was separated from an earlier clockwise vortex D0 during the first half of this rightward stroke. Vortex D0 became a shed vortex which was left behind the moving cylinder and is now located near $(x/D, y/D) \approx (-2.5, -0.5)$. On the upper surface of the cylinder, there is a more mature counterclockwise vortex B1 which has been growing from the rollup of the upper shear layer almost from the start of the present rightward stroke. At $t^*=2/16$, shedding of B1 is observed and its detachment from the cylinder surface is concurrent with the upward migration of A1 into the space in between. Upon shedding, vortex B1 is located near $(x/D, y/D) \approx (0.5, 0.5)$.

Similar to a vortex in mode I, vortex A1 is migrated upward around the trailing surface of the cylinder on approaching its rightmost position [Fig. 7(b)]. When the cylinder reverses its stroke, A1 has been completely migrated to the upper cylinder surface and continues to be fed with negative vorticity from the now leftward-moving cylinder. At $t^*=6/16$, the returning cylinder meets vortex B1 again and vortex A1 is observed to be stretched in the x direction probably due to the fluid circulation of B1 [Fig. 7(d)]. A strong secondary flow stream can be observed flowing between the two vortices and upward along the 45° direction. In Fig. 7(e), A1 is stretched into two parts when it moves underneath B1. The trailing part is left behind the cylinder as the shed vortex A1 where the part remained attached to the moving cylinder continues to grow as the next clockwise vortex D1.

After A1 is shed, it pairs up with B1 to form a vortex pair in Fig. 7(f). At this phase of $t^*=8/16$, the cylinder moves with its maximum speed past its neutral position. Under the effect of the secondary flow stream and probably also under the combined induced flow of the vortices, the vortex pair starts to convect away from the line of cylinder motion along the 45° direction. The convection of the vortex pair is clearly evident from the sequences of PIV snapshots from $t^*>7/16$ in Figs. 7(f)–7(h). As the vortex pair convects farther away from the line of cylinder motion, the shed vortices show obvious reduction in their peak vorticity levels. This weakening of vortical motion has been observed on a vortex when it is shed from a circular cylinder and thus cuts off from the supply of vorticity from a shear layer.[24]

Returning to the moving cylinder, the clockwise vortex D1 follows the same development stages as vortex A1 except that its growth starts on the upper cylinder surface and in a leftward cylinder stroke. It is migrated from the upper cylinder surface to the lower surface when the cylinder completes the leftward stroke and starts the following rightward stroke [Figs. 7(f)–7(h)]. The migration is aided by the shedding of the counterclockwise vortex C1 from the lower side of the cylinder in Fig. 7(g). When the cylinder reverses its movement and travels to the right, vortex D1 is stretched and

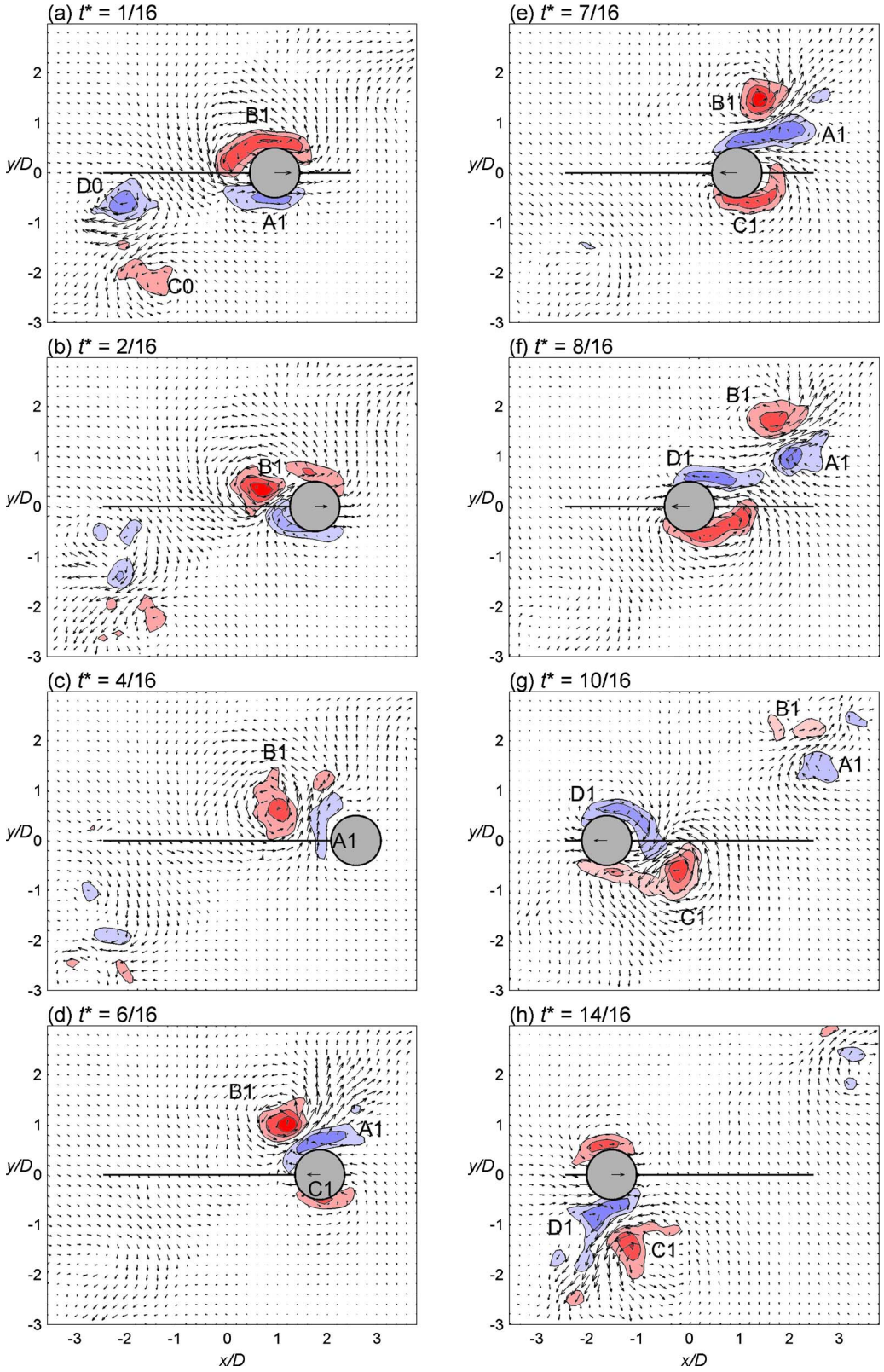

FIG. 7. (Color online) Mode II at KC=16: instantaneous PIV velocity vectors and vorticity contours at successive phases of cylinder movement. Vectors are shown on coarser grid for clarity. Instantaneous cylinder velocity is shown on cylinder in each plot. Cylinder speed at $t^*=8/16$ is U_m. Vorticity contours in $\omega_z^*=\pm 1.5, \pm 3.0, \pm 4.5, \ldots$.

separated into two parts under the effect of the nearby counterclockwise vortex C1. Figure 7(h) shows that the shed part of D1 and C1 form a vortex pair located at $y<0$ and to the left of the neutral cylinder position, that is, located at the third quadrant $(x<0, y<0)$. This vortex pair is next to the previous pair (C0 and D0) formed in the preceding cycle, which can be observed in Fig. 7(a). The predecessor of D1 is vortex D0, which has been separated into vortex D0 and A1

under the effect of vortex C0. Both vortex pairs convect away from the line of cylinder motion along the −135° direction.

Now we return to Fig. 7(d) at $t^*=6/16$. While vortex A1 undergoes interaction with vortex B1, a new clockwise vortex C1 rolls up from the lower shear layer of the leftward-moving cylinder. The following PIV snapshots show that for most of this leftward stroke, there is no vortex below the line of cylinder motion ($y<0$) to interact with vortex C1. Thus it develops in a similar way as a vortex behind a cylinder in a constant-speed cross flow. Unlike most vortices described earlier, there is no evidence of any significance migration of C1 around the cylinder surface. It grows for a time roughly about 3/4 stroke length before being shed near $t^*=10/16$ in Fig. 7(g). The shedding is concurrent with the intrusion of D1 from the upper side of the cylinder and a secondary flow stream flowing downward at about −135° to the $+y$ axis. This secondary flow stream is clearly connected with the dynamics and interaction of vortices C1 and D1. The convection of the vortex pair away from the line of cylinder also follows the secondary flow stream.

As the cylinder traverses its rightward stroke, a new counterclockwise vortex is rolled up from the upper shear layer. The vortex can be observed in Fig. 7(h), which is the successor of vortex B1 in the previous cycle. Similar to C1, this vortex (B1) develops all the way on the same (upper) side of the cylinder. It is shed after about 3/4 stroke length [Fig. 7(b)] and pairs up later with the next clockwise vortex (A1). The shedding and pairing of this vortex pair, all in the first quadrant ($x>0, y>0$), occur when the cylinder is located to the right of its neutral position. The dynamics is associated with the formation of a secondary flow stream along the 45° direction.

The development of vortices in mode II is summarized with a schematic sketch in Fig. 8. In a cylinder oscillation cycle, two vortex pairs are formed. Corresponding to the vortex pattern in Fig. 7, one vortex pair is formed and convecting in the first quadrant and the other pair in the third quadrant. They are separately connected with two secondary flow streams which flow away from the line of cylinder motion in two opposite directions along the 45°/−135° line. It is noted that in both vortex pairs, the counterclockwise vortex is on the obtuse angle side between the line of cylinder motion and the convection direction of the vortex pairs [Fig. 1(c)] while the vortex on the acute angle side has clockwise rotation. The two types of vortices are found to follow different sequences of development stages.

The counterclockwise vortex on the obtuse angle side, vortex B1, for example, undergoes a more natural growth on the same upper side of the cylinder from rollup to shedding (Fig. 8). The growth time starts shortly after the start of a stroke and ends at about 3/4 stroke length when shedding occurs. The clockwise vortex A1 undergoes a more complicated development. Similar to the vortices in mode I, vortex A1 undergoes a migration from one shear layer of the cylinder to the other. However, its initial formation and shedding are caused by stretching and separation of a region of vorticity concentration. This complex interaction takes place shortly after the cylinder starts a new stroke. At about 1/4

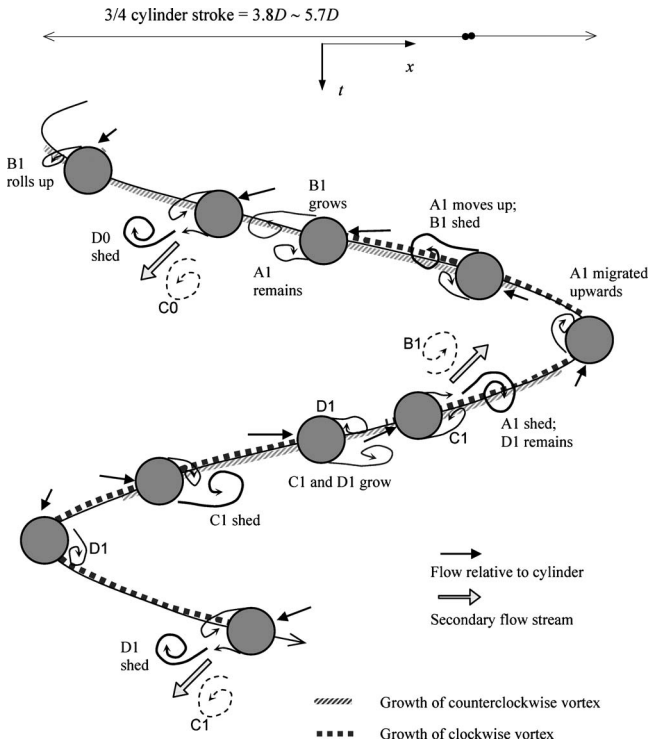

FIG. 8. Vortex development stages in mode II.

stroke length, vortex A1, which was formed in the previous stroke, has been migrated around the cylinder and switched to be connected with the other shear layer. When the cylinder drags the vortex past the fluid circulation of vortex B1, the vorticity region of A1 is stretched and eventually split into two parts, one as a shed vortex and the other remained attached to the shear layer. Together with B1, the shed vortex A1 forms a vortex pair in the first quadrant. The remaining vortex continues to grow and will end up as one partner of the other vortex pair in the third quadrant.

The separation of the vorticity region into two vortices has not been reported previously for the present flow. This is probably because most previous studies were based on flow visualizations in which interaction of vortices visualized as regions of dye concentration is difficult to interpret. Here, we show the detail stretching mechanism of the clockwise vortex in Fig. 9. This mode II pattern occurs at KC=20 but almost the same vortex dynamics occurs at the corresponding phases of cylinder oscillation at KC=16. Velocity vectors relative to the moving cylinder at the phases $t^*=7/16$ and 8/16 are shown in Figs. 9(a) and 9(b), respectively. The corresponding absolute velocity vector maps, not shown for brevity, are almost identical to those in Figs. 7(e) and 7(f), respectively, for KC=16, and thus we denote the vortices by the same names. The stretching of the vorticity region of A1 and the subsequent separation into vortices A1 and D1 are clearly observed under the effect of vortex B1 as the cylinder drags the attaching vortex past it. The relative vectors in Fig. 9 also suggest that the shedding of A1 from the splitting of the stretched negative vorticity region is not only induced by the fluid circulation of vortex B1 but also assisted by the intrusion of vortex C1 from below. If we ignore the presence

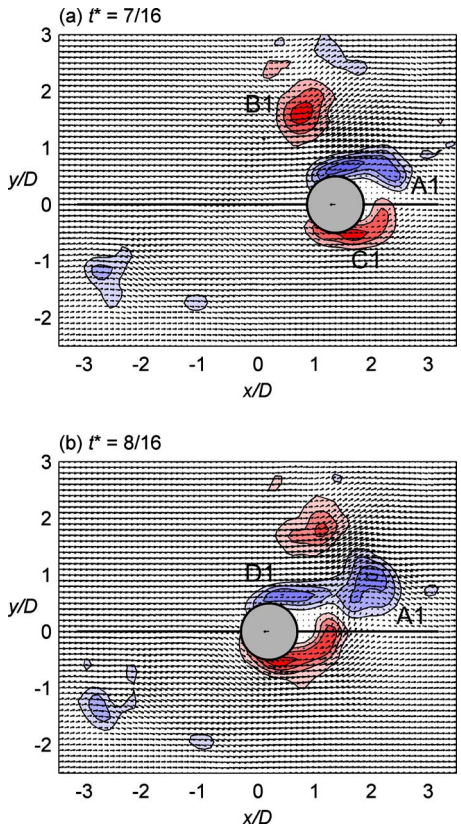

FIG. 9. (Color online) Vortex interaction in mode II. KC=20. PIV velocity vectors relative to moving cylinder around instant of vortex shedding. Maximum cylinder speed U_m is shown on cylinder in (b). Vorticity contours in $\omega_z^* = \pm 1, \pm 2, \pm 3, \ldots$.

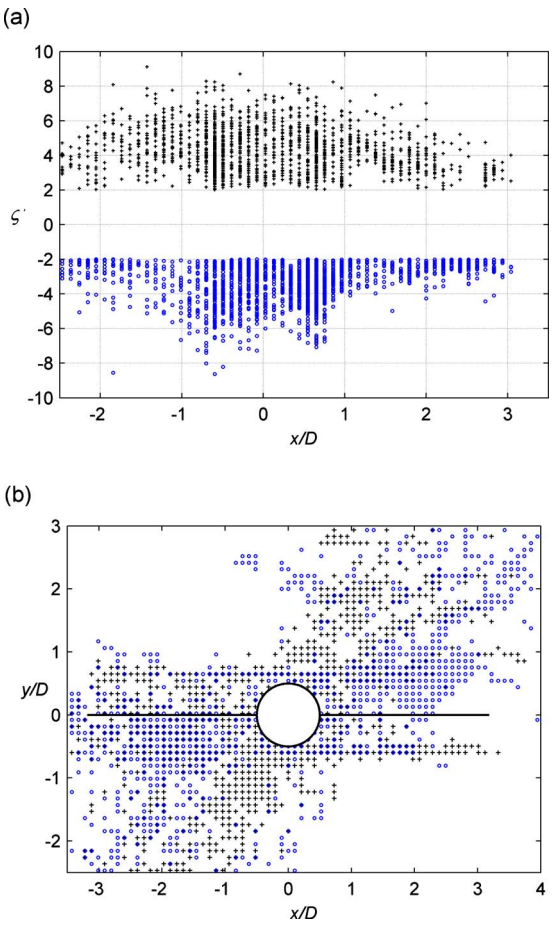

FIG. 10. (Color online) Ensemble of peak vorticity data from about 1000 PIV snapshots over a few cylinder oscillation cycles in mode II. KC=20: (a) peak vorticity levels; (b) locations of peaks. Symbols: +, positive vorticity; ○, negative vorticity.

of B1, the vortex dynamics revealed by the relative velocity vectors in Fig. 9(b) bears close resemblance to those of vortex shedding from a bluff body in a constant-velocity cross flow.[24,25]

Mode II is observed at KC between 16 and 24. As described in Figs. 7 and 8, the counterclockwise vortex, such as B1 or C1, develops over the first 3/4 of a stroke approximately. This distance is between 3.8*D* and 5.7*D* for KC between 16 and 24. It is believed that being always attached to the same shear layer, the vortex grows to the shedding stage in a natural manner. On the other hand, growth of the clockwise vortex spans over two successive strokes. Its initial formation and shedding are triggered by interaction with the counterclockwise vortex. The formation time for this vortex is from roughly the middle of a stroke to about the first quarter (or 3/8) of the following stroke. Although this development time at about 3/4–7/8 stroke length is slightly longer than that of the counterclockwise vortex, the development of the clockwise vortex is more complicated involving migration to the other side of the cylinder, stretching and separation into two vortices. As a result, the clockwise vortex, such as A1 and D1, is found to have weaker strength than the counterclockwise vortex.

For a statistical analysis, the center locations and strengths of large-scale vortices in the flow field are extracted in each PIV snapshot by the technique of identifying vorticity peaks.[25] The results for KC=20 are presented in Fig. 10 where all ensembles of vortex centers and peak vorticity levels from over some 1000 PIV snapshots covering three successive cylinder oscillation cycles are shown. It is evident from Fig. 10(a) that the counterclockwise vortices generally have higher magnitudes of peak vorticity levels than the clockwise vortices. The locations of vortex centers in Fig. 10(b) show clearly the double vortex street pattern. At this KC=20, the vortex formation time of 3/4 stroke length for the counterclockwise vortex equals 4.8*D*, which is the normal time for vortex formation.[1]

C. Transition between mode I and mode II

We have focused our attention mainly on the results at KC=16 because both submodes of mode I and mode II are observed at this KC. It is often observed during the experiments that mode II will transit into the inclined vortex street submode of mode I, or the other way round, within a few cylinder oscillation cycles. Figure 11 shows the flow at a cycle of mode I which exhibits some tendency to transition. In Fig. 11(a), the cylinder is toward the end of a leftward stroke. The vortex pair, which is shed earlier in this stroke, can be observed as A0 and B0 at locations away from the line of cylinder motion. The counterclockwise vortex A1, which grows during this stroke, is migrated from the lower

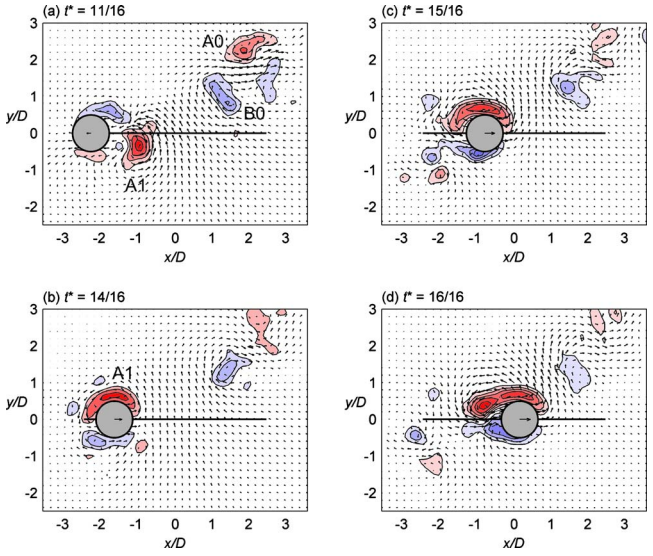

FIG. 11. (Color online) Mode transition at KC=16. Maximum cylinder speed U_m is shown on cylinder in (d). Vorticity contours in $\omega_z^* = \pm 1, \pm 2, \pm 3, \ldots$.

shear layer to the leeward side of the moving cylinder. The vortex pattern at this phase is similar to that in Fig. 3(e), but here, A1 undergoes development at a slightly faster pace so that it appears to be already shed from the cylinder at this instant. However, shedding occurs very close to the end of the stroke and the vortex has already migrated upward toward the line of cylinder movement. Thus, when the cylinder returns on the rightward stroke in Fig. 11(b), it can still bring the vortex upward to its upper surface as a mode I vortex. However, unlike the case in Fig. 3(g), not the entire A1 is brought over. It can be observed from the flow vectors and vorticity contours in Figs. 11(b) and 11(c) that a fraction of the positive vorticity region becomes detached from the main vortex A1 and remains on the lower side of the line of cylinder motion. As the cylinder moves onward to the right, this small vortex is shed or left behind. Moreover, it appears to induce a small region of negative vorticity to detach from the rolled up lower shear layer of the rightward-moving cylinder. This results in a small vortex pair located in the third quadrant of the flow field [Fig. 11(d)]. The vortex pair is associated with low levels of vorticity and a very weak secondary flow stream along the $-135°$ direction.

If vortex A1 in Fig. 11 becomes mature and sheds at an earlier location during the leftward stroke, its entire vorticity region will not be migrated above the line of cylinder motion. Instead, similar to Fig. 7(g), the clockwise vortex rolled up from the upper shear layer will be migrated downward before the cylinder reaches the end of the stroke (which is initiated by its downward intrusion to facilitate the shedding of A1). Then another vortex pair will be shed in the third quadrant and the vortex pattern changes to mode II. The results in Fig. 11 provide evidence to support the governing role of the stroke length (which is directly proportional to KC) and the resulting distance for growth of a vortex in determining the modes of vortex patterns.

D. Mode III pattern

As KC number increases more (KC≥24), mode III is observed. One longitudinal vortex street, similar to a von-Karman street of finite length, is formed behind the cylinder in each cylinder stroke [Fig. 1(d)]. The vortex pattern resembles that behind a cylinder being towed at uniform velocity in quiescent water. At KC=24, three vortices are generated for each half cycle. Similar to previous studies, our results support that one more vortex is produced as KC number increases by 8, approximately. For instance, four vortices are shed from the cylinder for each stroke at KC=32–36. As suggested by Obasaju *et al.*,[6] more submodes may be named with the increase in KC number. Nevertheless, the common feature is that the street is neither lateral nor oblique to the cylinder motion. The vortex street always lies along the line of cylinder motion and the vortex formation stages are different from and less complex than those in modes I and II. Therefore, we name all vortex patterns at KC≥24 as mode III.

In this mode, the vortices shed in the previous stroke may be present on the path of the returning cylinder, resulting in vortex impingement, splitting, or dislocation. Consequently, the flow structures of mode III are less regularly organized as compared with those of mode I or II. As an example, a sequence of PIV snapshots for mode III is shown in Fig. 12. When the cylinder passes its neutral position in a rightward stroke at $t^*=1/16$, the velocity vectors and vorticity contours in Fig. 12(a) show that two vortices have been shed behind the cylinder. A mature counterclockwise vortex P, which has been rolled up from the upper shear layer, is about to be shed. Shortly before the cylinder reaches its rightmost position at $t^*=4/16$, vortex P is shed [Fig. 12(b)]. Now the cylinder reverses its direction and starts the leftward stroke. The shear layers on both the upper and lower cylinder surfaces start to roll up and two regions of vorticity concentration can be observed there at $t^*=5/16$ in Fig. 12(c). The cylinder then meets vortex P and interaction occurs. The interaction takes the probable form of induction and amalgamation of counterclockwise fluid circulation between vortex P and the newly formed counterclockwise vortex A on the lower shear layer of the cylinder. For a clearer observation of the interaction mechanism, Fig. 13(a) shows the flow relative to the moving cylinder at this phase. It is evident that vortex P is attracted toward vortex A by the flow vectors. Although at this phase, the cylinder has just accelerated from the rest for a short distance from its rightmost extreme position, the long cylinder stroke and this large KC number give rise to a significant cylinder velocity for the vortex interaction. The impingement of the cylinder onto vortex P also appears to break off a small region of positive vorticity concentration from the vortex into the wake above the cylinder.

When the cylinder moves farther to the left, the PIV results in Fig. 12(d) suggest that the interaction between vortices P and A leads to a larger strength of the latter as compared with the clockwise vortex B rolled up from the upper shear layer. As a result, vortex A becomes the first vortex shed during this leftward stroke. The shedding takes place when the cylinder is near its neutral position. In the latter

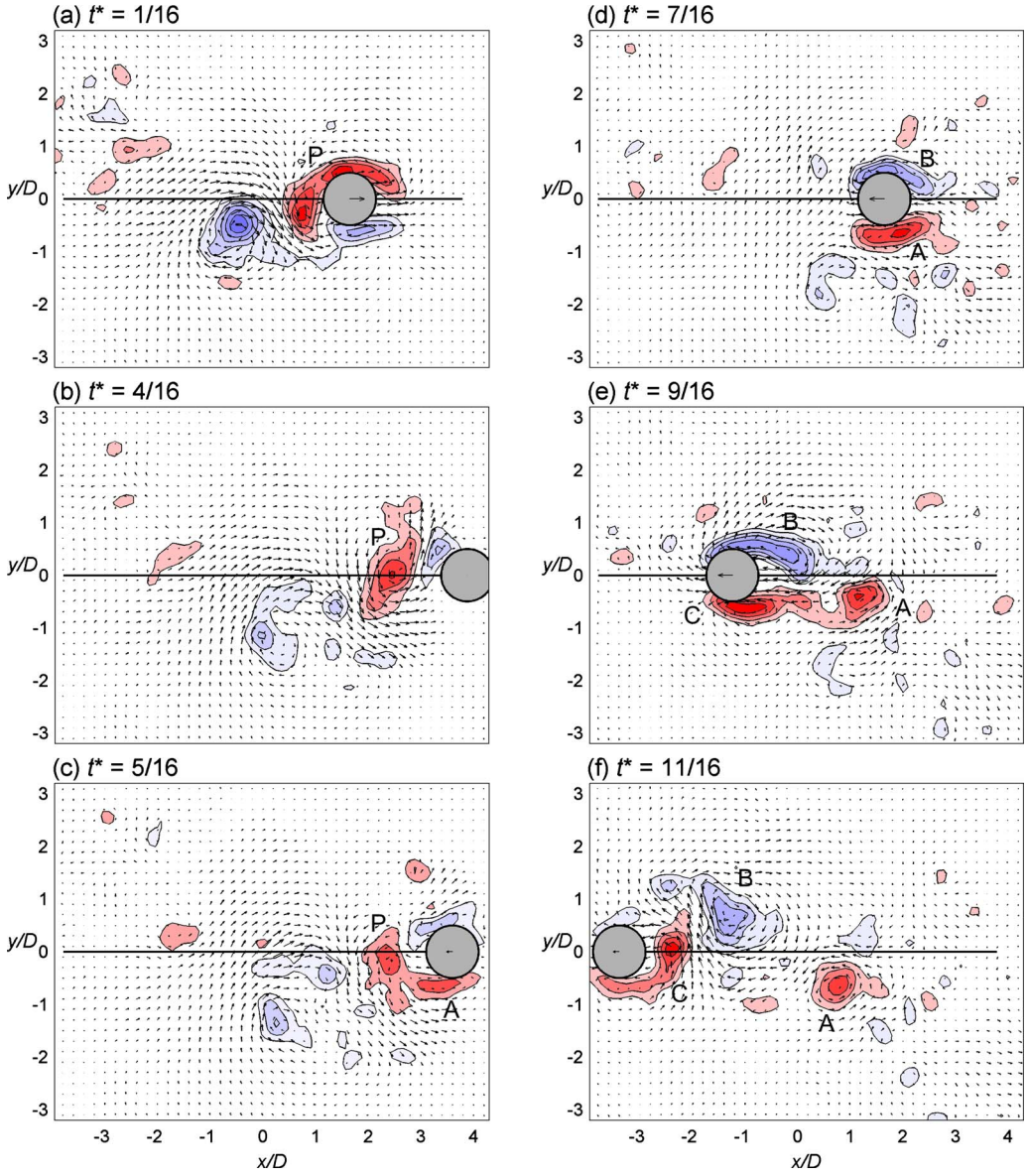

FIG. 12. (Color online) Instantaneous PIV velocity vectors and vorticity contours at successive phases of cylinder movement of mode III at KC=24. Vectors are shown on coarser grid for clarity. Instantaneous cylinder velocity is shown on cylinder in each plot. Cylinder speed at $t^*=1/16$ is $0.924U_m$. Vorticity contours in $\omega_z^*=\pm 0.8, \pm 1.6, \pm 2.4, \ldots$.

part of the stroke, vortex B and the next counterclockwise vortex C are shed. Their shedding mechanism is similar to that behind a cylinder in a constant velocity cross flow. This is supported by the relative flow vector map in Fig. 13(b), which bears close resemblance to constant-speed flow past a circular cylinder.[22]

In terms of the vortex formation distance, vortex A grows from the start to the middle of the stroke, that is approximately a distance of $3.8D$ at KC=24. The clockwise vortex B also grows from the start of the stroke but is shed later at about 5/8 stroke length. This is equivalent to the natural vortex formation length of $4.8D$, suggesting that vortex B develops in a natural manner. Vortex C has a similar vortex formation length as vortex A. In this cycle of Fig. 12, the three vortices shed in either the leftward or rightward stroke consist of two counterclockwise vortices and a clockwise vortex in between. This means that over all cycles in which this geometry persists, a clockwise vortex is always found near the center of the cylinder traverse while fluid circulation of the counterclockwise sense is always found near the two extreme positions of the cylinder traverse.

The normal vortex formation distance suggested in Jeon and Gharib[1] is $4.8D$. Mode III pattern starts with three vortices shed in one cylinder stroke such as that in Fig. 12. In a vortex street pattern, a vortex starts to grow near the middle growth stage of the previous contrarotating vortex. Thus a distance of two times $4.8D$ or $9.6D$ is sufficient for the normal growth of three successive vortices in a street pattern. A stroke length of $9.6D$ corresponds to KC=30.2. This explains the range of KC between 24 and 32 for the mode III pattern of three vortices per half cycle. The distance for the normal growth of four vortices from alternating sides of the cylinder will be $12D$. The corresponding KC is 37.7, which is in the middle of the expected range of KC between 32 and

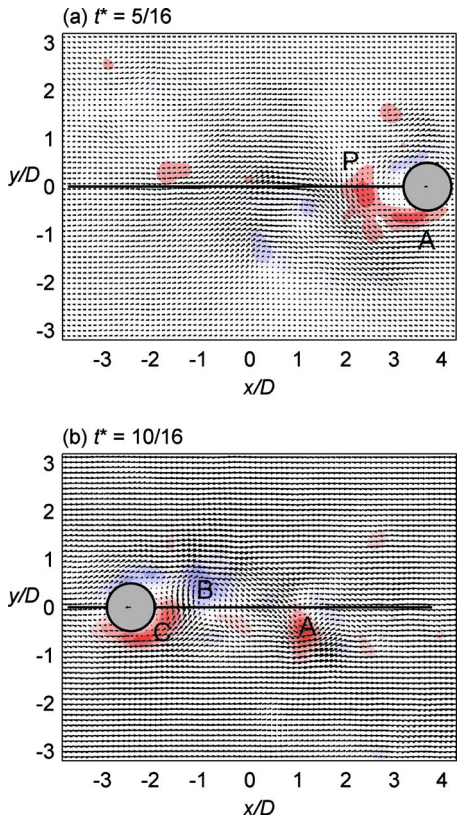

FIG. 13. (Color online) PIV velocity vectors relative to moving cylinder. Mode III at KC=24. Refer to Fig. 12 for vorticity levels.

40. For five vortex pairs in a cycle, the stroke length for normal vortex growth will be 14.4*D*, which is equivalent to KC=45, and the expected KC range is between 40 and 48.

E. Vortex pattern and secondary flow stream

Our results show that each vortex pattern is coupled with its own type of secondary flow stream around the cylinder.[9] The secondary flow stream is believed to be driven by fluid circulation of the vortices and associated pressure distribution in the flow field. For mass conservation, water flows from the surrounding ambient environment to supply the secondary flow stream (Fig. 1). On the other hand, the secondary flow stream and the associated ambient water flow keep the vortex pattern quasistable for a number of cycles before transition occurs.

For the inclined vortex street submode of mode I, the secondary flow stream is inclined at roughly 45° to the line of cylinder motion and moves away from the cylinder [Fig. 1(b)]. The majority of the secondary stream occurs on one side of the line of cylinder motion only, with a small fraction flowing in the opposite direction on the other side. The magnitude of the stream reduces as the distance from the cylinder increases, which is expected. On the side with the vortex street, ambient water flows toward the secondary flow stream in nearly normal directions. It is worth noting that ambient water flow is largely observed on the left side of the cylinder [for the vortex pattern in Fig. 1(b)]. The secondary flow stream in the lateral vortex street submode behaves in a similar manner, except the orientation of the vortex street to the line of cylinder motion [Fig. 1(a)].

In mode II, both the secondary stream and ambient water flow occur on both sides of the line of cylinder motion and exhibit an approximately antisymmetric pattern about the line [Fig. 1(c)]. In other words, they occur in two opposite quadrants at 45° with respect to the line of cylinder motion. In the figure, ambient water flows downward on the left side of the cylinder, replenishing the secondary flow stream at $y<0$, whereas ambient water on the right side flows upward. Velocities at locations nearer the cylinder, either at $x>0$ or $x<0$, are relatively larger in magnitudes, probably due to lower pressure that resulted from cylinder movement and vortex shedding.

The flow around the oscillating cylinder in mode III is very similar to that behind a towed cylinder.[26] Figure 1(d) sketches the flow when the cylinder moves to its leftmost position during which the secondary flow stream moves leftward behind the cylinder. Ambient water flows toward the line of cylinder motion as it is entrained into the street by the coherent motion of the vortical structures. When we follow the locations of the shed vortices in Fig. 12, it becomes evident that the secondary flow stream plays a role in convecting the shed vortices in the direction of cylinder movement in that stroke. When the cylinder reverses its direction, the secondary stream and the ambient water change flow direction accordingly.

IV. CONCLUSIONS

We apply time-resolved PIV measurements to investigate the characteristics and formation mechanism of vortex patterns around a circular cylinder undergoing sinusoidal oscillation in quiescent water. Keeping a constant Reynolds number at Re=2400, KC number is varied from 8 to 36. Similar to previous studies, three typical vortex patterns are identified which we name as modes I, II, and III. The modes are characterized by one, two, and three (or more) vortices generated, respectively, for each half cycle. Mode I is further separated into two submodes of a lateral vortex street and an inclined vortex street. Each vortex pattern is coupled with one typical pattern of water flow around the cylinder. The results show that KC number, or equivalently, the stroke length of cylinder motion, and the secondary flow stream are the key factors responsible for the different vortex patterns.

The vortices in mode I, which occurs at KC=8–16, are present only on one side of the line of cylinder motion. A vortex is shed always from the same one side of the cylinder near the middle of each stroke (Fig. 5). The sense of rotation of the vortex depends on the direction of the cylinder stroke. Hence, vortices of alternating senses of rotation are shed over successive cylinder strokes and they convect to one side of the line of cylinder motion in the form of either a lateral or an inclined vortex street. Each vortex is actually first rolled up from the shear layer on the other side of the cylinder in the previous cylinder stroke. The vortex undergoes a migration to the side of the cylinder with the vortex street. The migration seems to be compatible with the instantaneous

relative flow approaching the cylinder as a result of the prevailing secondary flow stream and the changing cylinder velocity. There is also evidence from our PIV results that the initial migration of the vortex is associated with the intrusion of this new vortex toward the opposite shear layer to cut off the mature vortex there from its shear layer, and thus triggering the shedding of that vortex.

The vortex formed in each cylinder stroke follows the same stages of development and the growth lasts for one stroke and the first part of the next stroke. This "vortex formation distance or time" at KC between 8 and 16 is compatible with the value of 4.8*D* suggested in Jeon and Gharib[1] for the natural growth of vortex to be shed from a circular cylinder. The shedding of the vortex in mode I is thus explained by its growth to the critical circulation but there is also evidence that the shedding is triggered by vortex interaction when the cylinder passes over the previously shed vortex which has been left behind nearby. At KC near 12, the stroke length allows appropriate vortex formation time for natural growth of the vortex formed in each cylinder stroke. This may explain the occurrence of highly organized and periodic vortex pattern in form of a lateral vortex street around this value of KC, which has been reported in many previous studies. At higher KC, the inclined vortex street submode occurs more frequently. The alternating vortices in the inclined street appear to possess different strengths.

In mode II, there are two vortex streets on both sides of the line of cylinder motion and they are inclined about 45° to the cylinder motion. This mode is the dominant vortex pattern when KC falls in the range between 16 and 24. In each cylinder stroke, two vortices are shed at different instants and from the two different sides of the cylinder (above or below the line of cylinder motion). Over two successive cylinder strokes, two consecutive vortices with opposite senses of rotation are shed from the same side of the cylinder, thus forming a vortex pair (Fig. 8). In the vortex pair, the vortex on the obtuse angle side of the vortex street develops on the same side of the cylinder from rollup to shedding. It is found to possess higher levels of peak vorticity than its partner on the acute angle side, which is observed to undergo a more complicated sequence of development stages. The development is similar to that of a vortex in mode I, but in addition to the migration from one side of the cylinder to the other, the vortex also experiences vortex stretching and splitting (Fig. 9).

Mode III features one longitudinal vortex street, similar to a limited-length von-Karman street, which consists of at least three vortices. This mode occurs when $KC > 24$. One more vortex is produced in each half cycle with the increase in KC by 8, approximately. At KC between 24 and 32, three vortices are shed in each cylinder stroke but we found that they are not exactly in pairs. Instead, the first vortex shed in each stroke has the same sense of rotation as the third and last vortex shed in the previous stroke.

ACKNOWLEDGMENTS

The investigation is supported by a research grant awarded by the Research Grants Council of Hong Kong (Grant No. HKU7144/05E).

[1] D. Jeon and M. Gharib, "On the relationship between the vortex formation process and cylinder wake vortex patterns," J. Fluid Mech. **519**, 161 (2004).
[2] P. Scandura, G. Vittori, and P. Blondeaux, "Three-dimensional oscillatory flow over steep ripples," J. Fluid Mech. **412**, 355 (2000).
[3] D. J. Maull and M. G. Milliner, "Sinusoidal flow past a circular cylinder," Coast. Eng. **2**, 149 (1978).
[4] P. W. Bearman and I. G. Currie, "Pressure-fluctuating measurements on an oscillating circular-cylinder," J. Fluid Mech. **91**, 661 (1979).
[5] P. W. Bearman, J. M. R. Graham, and S. Singh, "Forces on cylinders in harmonically oscillating flow," in *Mechanics of Wave Induced Forces on Cylinders*, edited by T. L. Shaw (Pitman, London, 1979).
[6] P. W. Bearman, M. J. Downie, J. M. R. Graham, and E. D. Obasaju, "Forces on cylinders in viscous oscillatory flow at low Keulegan–Carpenter numbers," J. Fluid Mech. **154**, 337 (1985).
[7] C. H. K. Williamson, "Sinusoidal flow relative to circular cylinders," J. Fluid Mech. **155**, 141 (1985).
[8] E. D. Obasaju, P. W. Bearman, and J. M. R. Graham, "A study of forces, circulation and vortex pattern around a cylinder in oscillating flow," J. Fluid Mech. **196**, 467 (1988).
[9] M. Tatsuno and P. W. Bearman, "A visual study of the flow around an oscillating circular cylinder at low Keulegan–Carpenter numbers and low Stokes numbers," J. Fluid Mech. **211**, 157 (1990).
[10] P. Justesen, "A numerical study of oscillating flow around a circular cylinder," J. Fluid Mech. **222**, 157 (1991).
[11] H. L. Zhang and X. Zhang, "Flow structure analysis around an oscillating circular cylinder at low KC number: A numerical study," Comput. Fluids **26**, 83 (1997).
[12] H. Dütsch, F. Durst, S. Becker, and H. Lienhart, "Low-Reynolds-number flow around an oscillating cylinder at low Keulegan–Carpenter numbers," J. Fluid Mech. **360**, 249 (1998).
[13] J. C. Lin and D. Rockwell, "Horizontal oscillations of a cylinder beneath a free surface: Vortex formation and loading," J. Fluid Mech. **389**, 1 (1999).
[14] K. M. Lam and G. Q. Dai, "Formation of vortex street and vortex pair from a circular cylinder oscillating in water," Exp. Therm. Fluid Sci. **26**, 901 (2002).
[15] T. Sarpkaya, "Experiments on the stability of sinusoidal flow over a circular cylinder," J. Fluid Mech. **457**, 157 (2002).
[16] Y. Yang and D. Rockwell, "Interaction of a deep-water wave with a vertical cylinder: Flow structure and loading," J. Fluid Mech. **520**, 267 (2004).
[17] T. Sarpkaya, "Structures of separation on a circular cylinder in periodic flow," J. Fluid Mech. **567**, 281 (2006).
[18] J. R. Elston, H. M. Blackburn, and J. Sheridan, "The primary and secondary instabilities of flow generated by an oscillating circular cylinder," J. Fluid Mech. **550**, 359 (2006).
[19] T. Sarpkaya, "Force on a circular cylinder in viscous oscillatory flow at low Keulegan–Carpenter numbers," J. Fluid Mech. **165**, 61 (1986).
[20] C. E. Willert and M. Gharib, "Digital particle image velocimetry," Exp. Fluids **10**, 181 (1991).
[21] K. M. Lam and M. Y. H. Leung, "Asymmetric vortex shedding flow past an inclined flat plate at high incidence," Eur. J. Mech. B/Fluids **24**, 33 (2005).
[22] B. Cantwell and D. Coles, "An experimental study of entrainment and transport in the turbulent near wake of a circular cylinder," J. Fluid Mech. **136**, 321 (1983).
[23] J. C. Lin and D. Rockwell, "Quantitative interpretation of vortices from a cylinder oscillating in quiescent fluid," Exp. Fluids **23**, 99 (1997).
[24] Y. Zhou and M. W. Yiu, "Flow structure, momentum and heat transport in a two-tandem-cylinder wake," J. Fluid Mech. **548**, 17 (2006).
[25] K. M. Lam, "Vortex shedding flow behind a slowly rotating circular cylinder," J. Fluids Struct. **25**, 245 (2009).
[26] M. M. Zdravkovich, *Flow Around Circular Cylinders. Vol. 1: Fundamentals* (Oxford University Press, New York, 1997).